Josephson Diode Effect in Supercurrent Interferometers

Rubén Seoane Souto,[1,2] Martin Leijnse,[1,2] and Constantin Schrade[1]
[1]Center for Quantum Devices, Niels Bohr Institute, University of Copenhagen, 2100 Copenhagen, Denmark
[2]Division of Solid State Physics and NanoLund, Lund University, S-22100 Lund, Sweden

(Received 15 May 2022; revised 10 October 2022; accepted 2 December 2022; published 22 December 2022)

A Josephson diode is a nonreciprocal circuit element that supports a larger dissipationless supercurrent in one direction than in the other. In this Letter, we propose a class of Josephson diodes based on supercurrent interferometers composed of Andreev bound state Josephson junctions or interacting quantum dot Josephson junctions, which are not diodes themselves but possess nonsinusoidal current-phase relations. We show that such Josephson diodes have several important advantages, like being electrically tunable and requiring only time-reversal breaking by a magnetic flux. We also show that our diodes have a characteristic ac response, revealed by the Shapiro steps. Even the simplest realization of our Josephson diode paradigm that relies on only two junctions can achieve efficiencies of up to ∼40% and, interestingly, far greater efficiencies are achievable by concatenating interferometer loops. We hope that our Letter will stimulate the search for highly tunable Josephson diode effects in Josephson devices based semiconductor-superconductor hybrids, $2d$ materials, and topological insulators, where nonsinusoidal current-phase relations were recently observed.

DOI: 10.1103/PhysRevLett.129.267702

Nonreciprocal circuit elements underlie many applications of semiconductor electronics, such as current rectifiers, power converters, and photodetectors. The most paradigmatic example of a nonreciprocal circuit element is the semiconductor diode that, conditioned on the polarity of a voltage bias, controls a *dissipative current* flow. Driven by the need for energy-efficient circuitry, there has recently been mounting interest in extending the concept of a semiconducting diode to a "Josephson diode" (JD) [1–27] that, depending on the direction of a current bias, supports a larger *dissipationless supercurrent* in one direction than in the other. Promising applications of such a JD could comprise superconducting (SC) electronic circuits with reduced power consumption and signal isolation in superconducting neural networks [28,29].

However, a difficulty toward realizing a JD is that the current-phase relation (CPR) in time-reversal or inversion-symmetric Josephson junctions (JJs) is symmetric around zero SC phase difference, $I(\varphi) = -I(-\varphi)$. This property ensures that the critical currents for the two current-bias directions, I_c^+ and I_c^-, are equal so that a JD effect is missing. To circumvent this constraint, previous Letters studied a diode effect in inversion-symmetry breaking superconducting thin films [1–6], JJs of finite-momentum superconductors [7–9], JJs of multilayered materials [10–14], topological insulator JJs [15,16], and spin-orbit coupled $2d$ electron gas JJs subject to a Zeeman field [17–19]. Moreover, it was noted that a diode effect can arise in spin-orbit coupled nanowire JJs subject to a Zeeman field [20–23], magnetic junctions [24–26], and domain wall SC channels [27].

In this Letter, we consider an alternative platform for a JD in a supercurrent interferometer containing two or more mesoscopic JJs, such as quantum material JJs hosting highly transmitting Andreev bound states or quantum dots. These JJs are not diodes themselves but

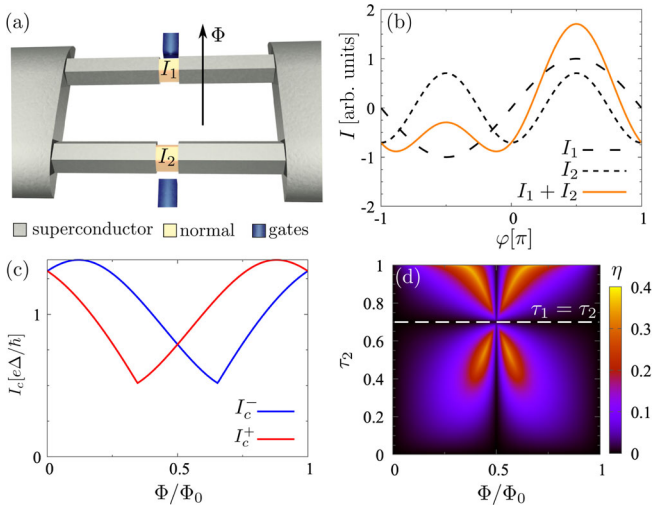

FIG. 1. (a) Minimal experimental setup for a JD interferometer comprising two JJs with nonsinusoidal CPRs. (b) Interference of different supercurrent harmonics $I_{\ell=1,2}$ that gives rise to the JD effect. (c) Critical currents for two current-bias directions $I_c^{\pm}$ in a quantum point contact interferometer versus external flux Φ. (d) Diode efficiency η of an Andreev interferometer versus external flux Φ and transmission τ_2 of the second JJ. The transmission of the first JJ is $\tau_1 = 0.7$.

have a high-harmonic content in their CPR. We show that such JDs have multiple advantages, such as being all-electrical tunable and requiring only time-reversal breaking by a magnetic flux. For characterizing the JD effect, we use the diode efficiency, defined as

$$\eta = \frac{\Delta I_c}{I_c^+ + I_c^-} \quad \text{with} \quad \Delta I_c = |I_c^+ - I_c^-|. \tag{1}$$

While we show that this diode efficiency can reach ∼40% for the single-loop interferometer with two JJs, we also propose a route for systematically increasing the diode efficiency by concatenating multiple interferometers. Finally, we show that the JD effect also manifests itself in the ac response of our setup as asymmetric Shapiro steps and we discuss applications of our JD paradigm for calibrating protected superconducting qubits [30–33].

Setup and minimal model.—Our setup comprises a pair of mesoscopic JJs ($\ell = 1, 2$) that connect two conventional SC leads to form a supercurrent interferometer (or superconducting quantum interference device, SQUID), see Fig. 1(a). To illustrate the origin of the JD effect in such an interferometer, we introduce a minimal model in which the CPRs of the two JJs include only a first harmonic and second harmonic contribution,

$$I_\ell(\varphi) = I_\ell^{(1)} \sin(\varphi) + I_\ell^{(2)} \sin(2\varphi). \tag{2}$$

Here, φ is the SC phase difference and $I_\ell^{(m)}$ is the amplitude of the mth harmonic for the ℓth JJ. Upon piercing an external magnetic flux Φ, through the area between the JJs, the total CPR of the interferometer reads

$$I(\varphi) = I_1(\varphi) + I_2(\varphi - 2\pi\Phi/\Phi_0). \tag{3}$$

Here, $\Phi_0 = h/2e$ denotes the magnetic flux quantum and we have assumed that self-inductance effects [34] are negligible, implying that (by fabrication) the only difference between the interferometer arms arises from the two JJs. The critical currents for the two current-bias directions are then given by $I_c^\pm = \max_\varphi[\pm I(\varphi)]$.

With this minimal model, we can now explain how the JD effect arises. For that purpose, we initially set $\Phi = \Phi_0/8$ and consider the case when one JJ comprises only a first harmonic $I_1(\varphi) \propto \sin(\varphi)$, while the other JJ comprises only a second harmonic $I_2(\varphi - 2\pi\Phi/\Phi_0) \propto \cos(2\varphi)$. As shown in Fig. 1(b), the two CPRs then interfere destructively for $-\pi < \varphi < 0$ and constructively for $0 < \varphi < \pi$. This interference effect, which behaves *opposite* for positive and negative SC phase differences, gives rise to unequal critical currents for the two current bias directions $I_c^+ \neq I_c^-$, and thus to a JD effect.

This conceptual picture of the JD effect's origin does not change qualitatively when adding additional harmonics to the JJ CPRs. In the previous situation when one JJ comprised only a second harmonic so that $I_2^{(1)} = 0$, the I_c^- critical current corresponded to one of two minima within the range $-\pi < \varphi < 0$, see Fig. 1(b). When gradually turning on, for example, a finite first harmonic so that $I_2^{(1)} > 0$, these two minima acquire different depth. However, the values of the global maximum and minimum of the CPR remain different and thus $I_c^+ \neq I_c^-$.

Andreev interferometer.—So far, our minimal model helped us develop a conceptual picture of the JD effect in supercurrent interferometers. A natural next step is to clarify the detailed experimental requirements for a JD. For that purpose, we will consider more realistic interferometer setups with JJs that comprise beyond-second harmonic contributions, extending the minimal model of Eq. (2). We first consider an interferometer with JJs for which Andreev bound states with gate-tunable transmissions mediate the supercurrent. Such Andreev bound state JJs have recently been realized in spin-orbit coupled semiconductor JJs [35,36], topological insulator JJs [37–39], or graphene JJs [40,41]. The CPR of an Andreev JJs is given by [42,43],

$$I_\ell(\varphi) = \frac{e\Delta^2\tau_\ell}{2\hbar}\frac{\sin(\varphi)}{\varepsilon_\ell(\varphi)}\mathrm{Tanh}[\varepsilon_\ell(\varphi)/2k_BT],$$
$$\varepsilon_\ell(\varphi) = \Delta\sqrt{1 - \tau_\ell \sin^2(\varphi/2)}. \tag{4}$$

Here, $\varepsilon_\ell(\varphi)$ are the Andreev levels that emerge within the SC gap Δ and that mediate the supercurrent. Moreover, τ_ℓ are the transmission of the ℓth JJ and T is the temperature. Henceforth, we will assume $k_BT \ll \Delta$. In this situation, the CPR of Eq. (4) is approximately sinusoidal for small transmissions, $I_\ell(\varphi) \propto \sin(\varphi)$ if $\tau_\ell \ll 1$. However, for large transmissions $\tau_\ell \lesssim 1$, the CPR gets increasingly "skewed," thereby acquiring higher harmonic content, $I_\ell(\varphi) = I_\ell^{(1)} \sin(\varphi) + I_\ell^{(2)} \sin(2\varphi) + \cdots$.

Returning to our question on the experimental requirements for the JD, we proceed by computing the diode efficiency of the Andreev interferometer as a function of the transmissions τ_ℓ and the external flux Φ. A representative result is depicted in Fig. 1(d). It shows that the JD diode efficiency η comprises four lobes with a maximum efficiency of ∼40%. Moreover, we find from the simulations that the JD requires only three simple requirements that need to be *simultaneously* satisfied: (1) The external flux should not be an integer multiple of the half flux quantum $\Phi \neq n\Phi_0/2$. If this condition is not satisfied, then $I(\varphi) = -I(-\varphi)$ and $I_c^+ = I_c^-$, implying that the JD effect vanishes, see Fig. 1(c). (2) The junction transmissions should not be equal, $\tau_1 \neq \tau_2$. If this condition is not satisfied, then the CPR has the property $I(\varphi) = -I(-\varphi + 2\pi\Phi/\Phi_0)$, implying $I_c^+ = I_c^-$. The vanishing diode efficiency when $\tau_1 = \tau_2$ is shown by the dashed line in Fig. 1(d). (3) At least one of the JJ needs to be highly transmitting. This requirement ensures a sizable higher harmonic content in the total CPR.

If such a higher harmonic content is negligible (compared to the magnitude of the first harmonics), then the JD effect is again missing.

Last, we note that at the special point when $\Phi = \Phi_0/2$ and $\tau_1 = \tau_2$, all odd harmonics vanish in the interferometer CPR, $I(\varphi) \propto \sin(2\varphi) + \cdots$. In this case, the interferometer can (if shunted by a large capacitor) realize a protected superconducting qubit that stores quantum information in states of opposite Cooper-pair parity [30–33]. An application of our proposed diode effect is thus the calibration of such protected superconducting qubits by mapping out the phase diagram of Fig. 1(d).

Interacting quantum dot interferometer.—We have seen in the previous section that a CPR with higher harmonic content due to highly transmitting Andreev bound states can give rise to a JD effect. In this section, we consider another established approach for realizing higher harmonics with a JJ composed of a spin-degenerate quantum dot (QD) with charging energy U that couples with tunneling amplitudes $t_{L/R}$ to SC leads with SC gap Δ. Such a QD JJ can reverse the supercurrent when a gate voltage tunes the offset charge n_g on the dot [44,45]. Close to the supercurrent reversal, single Cooper pairs tunnel with approximately equal amplitude in the forward and reverse direction. As a result, the net current due to single Cooper pair tunneling, corresponding to the first harmonic, is reduced. In this regime, it was observed that higher harmonics contributions become relevant [46,47].

Motivated by this alternative mechanism to generate higher harmonics, we consider a second realization of the supercurrent interferometer with one low-transmitting JJ and one QD JJ. We first compute, assuming the zero-bandwidth approximation in the leads [48,49], the CPR of the QD JJ. For the detailed model, see Ref. [50]. Our results are shown in Fig. 2(a). We find that the first harmonic is reduced close to the supercurrent reversal transitions, while the second harmonic exhibits an enhancement. If we now arrange the QD JJ and a JJ with transmission $\tau \ll 1$ in a supercurrent interferometer, the JD effect emerges again. We have computed the diode efficiency in Fig. 2(b). As expected, the diode efficiency is maximal near the supercurrent reversal transitions where first and second harmonics have comparable magnitudes.

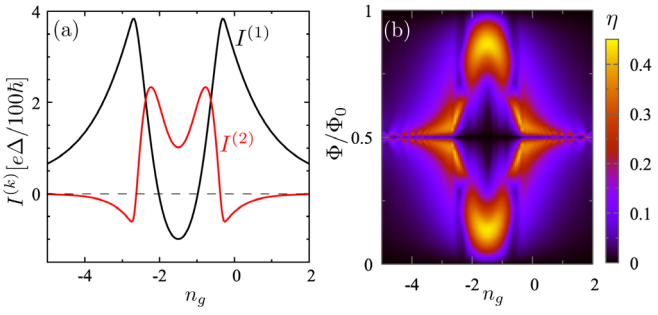

FIG. 2. (a) First and second harmonic $I^{(1,2)}$ of a QD JJ CPR with $(U, t_L, t_R, T) = (3, 2/3, 2/3, 0.001)\Delta$ versus offset charge, n_g. See Ref. [50] for the detailed model. (b) Diode efficiency η for an interferometer with a QD JJ and low-transmitting JJ versus flux Φ and offset charge n_g. Here, η is optimized with respect to the JJ transmission. QD parameters are as in (a).

Diode efficiency optimization.—Our previous JD implementations achieved efficiencies $\eta \sim 40\%$, see Figs. 1(c) and 2(b). We will now discuss how the diode efficiency can be optimized. One conceptual approach is to include additional harmonics in the CPR that elevate the critical current in one direction and reduce it in the reverse one. As an example, we return to Fig. 1(b) where $I(\varphi) \propto \sin(\varphi) - \cos(2\varphi)/\sqrt{2}$ and add a third harmonic $\propto -\sin(3\varphi)/\sqrt{3}$. This third harmonic will destructively and constructively interfere with the minima and maxima of the CPR, thereby enhancing the JD effect. Adding further harmonics so that $I(\varphi) \propto \sum_{n=1}^{N} \cos[n(\varphi - \pi/2)]/\sqrt{n}$ leads to a CPR that approaches asymptotically $\eta = 1$ for increasing N [50].

To implement this approach experimentally, we propose an array of parallel Andreev JJs arranged in an interferometer setup, see Fig. 3(a). We expect that tuning individually the interferometer fluxes and transmissions will create an optimized JD effect as discussed above. To find the maximum diode efficiencies, we use Monte Carlo maximization, randomly sampling the parameter space of transmissions and fluxes. We use $\sim 10^9$ sampling points, sufficient to find the maximum diode efficiency for $N_J \sim 10$ JJs. Results for the maximum efficiency are shown in Fig. 3(a) as a function of N_J. We find that the efficiency grows monotonously with N_J, increasing faster for small N_J. These results suggest that already a small number of concatenated loops is sufficient to significantly improve the diode efficiency.

However, we note that it is not possible to achieve perfect efficiency with a finite number of JJs, since there is no phase-independent term in a CPR. Hence, it is relevant to set bounds on the maximal efficiency achievable with N_J JJs that are not diodes themselves. Two JJs achieve the

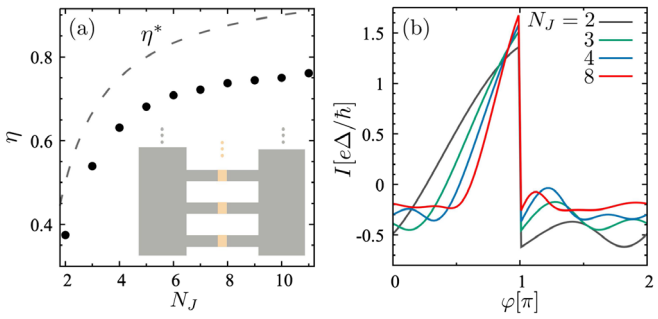

FIG. 3. (a) Maximum diode efficiency η for N_J JJs concatenated in an interferometer array (as shown in the inset). Dashed lines show $\eta^* = (N_J - 1)/N_J$. (b) CPR in the maximum diode efficiency configuration for various N_J.

highest diode efficiency when the supercurrent interference is optimal: the CPR maxima align, while the minimum of one junction aligns with the maximum of the other one. With this reasoning, the best upper bound we found is given by 50% for two JJs. By concatenating N_J JJs in the same way, the best upper bound we found for the diode efficiency is $\eta^* = (N_J - 1)/N_J$ [50].

Shapiro steps.—While we have so far explored the JD effect in dc-biased interferometers, it is natural to ask if there are also manifestations of the JD effect in an interferometer with *both* an applied dc bias *and* ac bias. To address this question, we consider for concreteness an interferometer with single-channel Andreev JJs. The time dependence of the phase difference $\varphi(t)$ and the voltage drop $V(t) = (\hbar/2e)\dot{\varphi}(t)$ is given by [56–58],

$$\frac{\hbar}{2eR}\dot{\varphi}(t) + I[\varphi(t)] = i_{\rm dc} + i_{\rm ac}\sin(\omega t). \tag{5}$$

Here, $i_{\rm dc}$ and $i_{\rm ac}$ are the amplitudes of the dc and ac bias. Moreover, ω is the driving frequency and R is a shunt resistance in parallel to the interferometer. For $I(\varphi) \propto \sin(\varphi)$, the primary consequence of Eq. (5) is the appearance of voltage plateaus or "Shapiro steps" in the $i_{\rm dc} - V$ curve when $V = V_n \equiv 2n\hbar\omega/e$. Here, n is an integer. We now want to understand how these Shapiro steps change for our JD interferometer.

To identify the possible changes of the Shapiro pattern for a JD interferometer, we have solved Eq. (5) numerically,

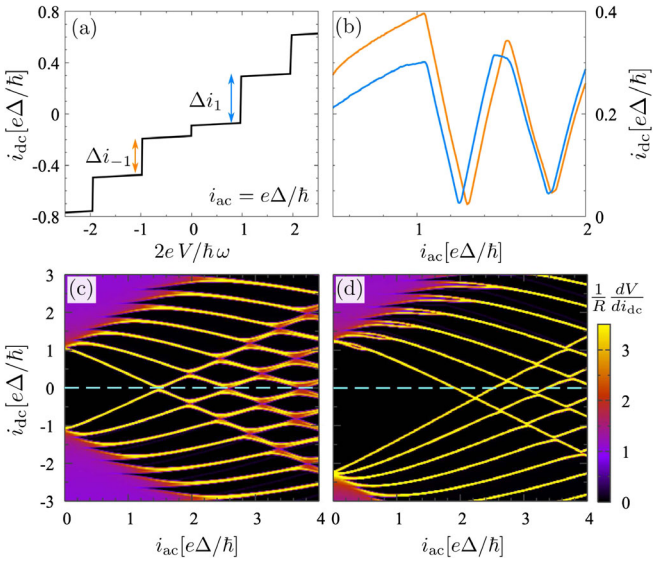

FIG. 4. (a) $i_{\rm dc} - V$ curve of an ac-biased Andreev interferometer, showing Shapiro steps with step heights Δi_n. (b) Step heights, $\Delta i_{\pm 1}$, as a function of $I_{\rm ac}$, showing a relative offset. (c) Differential resistance, $dV/dI_{\rm dc}$, versus $I_{\rm ac}$ and $I_{\rm dc}$, for an interferometer without JD effect, showing a symmetry around $I_{\rm dc} = 0$. (d) Same as (c) but for a interferometer with JD effect. The symmetry around $I_{\rm dc} = 0$ is missing. Parameters used for all plots are $(\tau_1, \tau_2, \Phi/\Phi_0, \omega) = (0.7, 0.99, 0.32, 0.2\Lambda)$ with $\Lambda = (2eR/\hbar)(e\Delta/\hbar)$, except (c) uses $\tau_2 = 0.7$.

leading to two notable findings: (1) In the $i_{\rm dc} - V$ curve of a conventional JJ with sinusoidal CPR, the step size (or plateau length in $i_{\rm dc}$) of the nth Shapiro step at $V = V_n$ is equal to the step size of the $-n$th Shapiro step, $\Delta i_n = \Delta i_{-n}$. This equality follows from the property $i_{\rm dc}(V) = -i_{\rm dc}(-V)$. In a JD interferometer, this no longer holds. As shown in Fig. 4(a), we find that the step sizes of the nth and $-n$th Shapiro steps are, in general, unequal, $\Delta i_n \neq \Delta i_{-n}$. This unusual behavior of the Shapiro step size becomes particularly apparent when tuning $i_{\rm ac}$, which shows oscillations with a relative offset between Δi_n and Δi_{-n}, see Fig. 4(b). (2) For a conventional JJ with no JD effect, a plot of the differential resistance $dV/di_{\rm dc}$ versus $i_{\rm ac}$ and $i_{\rm dc}$ shows a "fanlike" pattern with sharp peaks marking the Shapiro steps. As shown in Fig. 4(c), in the absence of the JD effect, the peaks in the differential resistance are mirror symmetric with respect to $i_{\rm dc} = 0$ and the separation between neighboring peaks on a fan (for fixed $i_{\rm ac}$) gives the Shapiro step size. In a JD interferometer, the differential resistance peaks lack the symmetry around $i_{\rm dc} = 0$, see Fig. 4(d). This unusual behavior arises due to the unequal critical currents for the two current-bias directions, so that the peaks emerge at different $i_{\rm dc}$ values for $i_{\rm ac} = 0$. Moreover, the separation between neighboring peaks is different for positive and negative dc current bias directions, which reconfirms our previous finding that $\Delta i_n \neq \Delta i_{-n}$.

Finally, we remark that earlier works have found that "fractional Shapiro steps" can arise in Andreev JJs at voltages $V = V_{n/m} \equiv 2(n/m)\hbar\omega/e$ due to the higher harmonic content in the CPR [59–61]. Interestingly, such fractional Shapiro steps can emerge in our setup in an even more pronounced way if $\tau_\ell \lesssim 1$. For example, by setting $\Phi = \Phi_0/2$ and tuning the JJs from an unbalanced ($\tau_1 \neq \tau_2$) to a balanced situation ($\tau_1 = \tau_2$), we find an *exact* doubling of the Shapiro steps, with all integer steps having the same height as half-integer steps, see Fig. 5. This exact doubling of Shapiro steps is due to a CPR with only even harmonics $I(\varphi) \propto \sin(2\varphi) + \cdots$, and could provide another way of calibrating protected superconducting qubits [30–33],

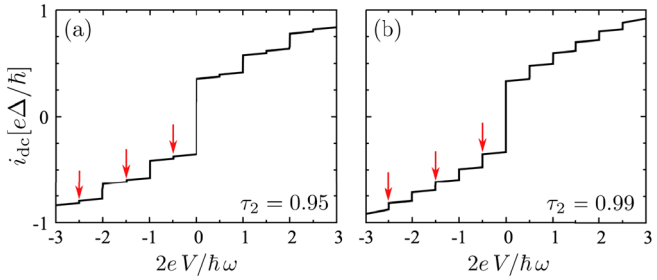

FIG. 5. Shapiro steps in the $i_{\rm dc}$-V curve for an dc- and ac-biased Andreev interferometer with drive amplitude $i_{\rm ac} = 0.4e\Delta/\hbar$ and $\Phi/\Phi_0 = 1/2$ (a) For $(\tau_1, \tau_2) = (0.99, 0.95)$, fractional Shapiro steps appear, highlighted by red arrows, which signal the importance of higher harmonics. (b) For $(\tau_1, \tau_2) = (0.99, 0.99)$, the fractional Shapiro steps have the same step heights as the integer Shapiro steps.

complementary to the method proposed in the section on the Andreev interferometer.

Conclusions.—We studied a JD effect in supercurrent interferometers of JJs with a nonsinusoidal CPR. We showed that such interferometers achieve sizable diode efficiencies, optimizable by concatenating interferometer loops. We also discussed a manifestation of the JD effect in the Shapiro steps and applications for qubit calibration. Exciting future directions may include the study of JDs with methods of circuit quantum electrodynamics when the flux Φ is replaced by a quantized field [62].

We acknowledge helpful discussions with J. M. Chavez-Garcia and M. Kjaergaard. We acknowledge funding from the Swedish Research Council (VR) and the European Research Council (ERC) under the European Union's Horizon 2020 research and innovation programme under Grant Agreement No. 856526, and NanoLund. We also gratefully acknowledge funding from the Microsoft Corporation.

Note added.—Recently, a manuscript [63] appeared, providing complementary analytical results on the JD effect for a variant of the minimal model of Eq. (2).

[1] F. Ando, Y. Miyasaka, T. Li, J. Ishizuka, T. Arakawa, Y. Shiota, T. Moriyama, Y. Yanase, and T. Ono, Nature (London) **584**, 373 (2020).
[2] L. Bauriedl, C. Bäuml, L. Fuchs, C. Baumgartner, N. Paulik, J. M. Bauer, K.-Q. Lin, J. M. Lupton, T. Taniguchi, K. Watanabe *et al.*, Nat. Commun. **13**, 4266 (2022).
[3] A. Daido, Y. Ikeda, and Y. Yanase, Phys. Rev. Lett. **128**, 037001 (2022).
[4] J. Shin, S. Son, J. Yun, G. Park, K. Zhang, Y. J. Shin, J.-G. Park, and D. Kim, arXiv:2111.05627.
[5] J. J. He, Y. Tanaka, and N. Nagaosa, New J. Phys. **24**, 053014 (2022).
[6] S. Ilić and F. S. Bergeret, Phys. Rev. Lett. **128**, 177001 (2022).
[7] B. Pal, A. Chakraborty, P. K. Sivakumar, M. Davydova, A. K. Gopi, A. K. Pandeya, J. A. Krieger, Y. Zhang, S. Ju, N. Yuan *et al.*, arXiv:2112.11285.
[8] M. Davydova, S. Prembabu, and L. Fu, Sci. Adv., **8** (2022).
[9] N. F. Yuan and L. Fu, Proc. Natl. Acad. Sci. U.S.A. **119**, e2119548119 (2022).
[10] H. Wu, Y. Wang, Y. Xu, P. K. Sivakumar, C. Pasco, U. Filippozzi, S. S. Parkin, Y.-J. Zeng, T. McQueen, and M. N. Ali, Nature (London) **604**, 653 (2022).
[11] J. Diez-Merida, A. Diez-Carlon, S. Y. Yang, Y.-M. Xie, X.-J. Gao, K. Watanabe, T. Taniguchi, X. Lu, K. T. Law, and D. K. Efetov, arXiv:2110.01067.
[12] J.-X. Lin, P. Siriviboon, H. D. Scammell, S. Liu, D. Rhodes, K. Watanabe, T. Taniguchi, J. Hone, M. S. Scheurer, and J. Li, Nat. Phys. **18**, 1221 (2022).
[13] H. D. Scammell, J. Li, and M. S. Scheurer, 2D Mater. **9**, 025027 (2022).
[14] Y. Zhang, Y. Gu, J. Hu, and K. Jiang, Phys. Rev. X **12**, 041013 (2022).
[15] A. Kononov, G. Abulizi, K. Qu, J. Yan, D. Mandrus, K. Watanabe, T. Taniguchi, and C. Schönenberger, Nano Lett. **20**, 4228 (2020).
[16] C.-Z. Chen, J. J. He, M. N. Ali, G.-H. Lee, K. C. Fong, and K. T. Law, Phys. Rev. B **98**, 075430 (2018).
[17] C. Baumgartner, L. Fuchs, A. Costa, S. Reinhardt, S. Gronin, G. C. Gardner, T. Lindemann, M. J. Manfra, P. E. Faria Junior, D. Kochan, J. Fabian, N. Paradiso, and C. Strunk, Nat. Nanotechnol. **17**, 39 (2021).
[18] C. Baumgartner, L. Fuchs, A. Costa, J. Picó-Cortés, S. Reinhardt, S. Gronin, G. C. Gardner, T. Lindemann, M. J. Manfra, P. E. F. Junior, D. Kochan, J. Fabian, N. Paradiso, and C. Strunk, J. Phys. Condens. Matter **34**, 154005 (2022).
[19] A. A. Reynoso, G. Usaj, C. A. Balseiro, D. Feinberg, and M. Avignon, Phys. Rev. B **86**, 214519 (2012).
[20] T. Yokoyama, M. Eto, and Y. V. Nazarov, J. Phys. Soc. Jpn. **82**, 054703 (2013).
[21] T. Yokoyama, M. Eto, and Y. V. Nazarov, Phys. Rev. B **89**, 195407 (2014).
[22] A. Zazunov, R. Egger, T. Jonckheere, and T. Martin, Phys. Rev. Lett. **103**, 147004 (2009).
[23] A. Brunetti, A. Zazunov, A. Kundu, and R. Egger, Phys. Rev. B **88**, 144515 (2013).
[24] S. Pal and C. Benjamin, Europhys. Lett. **126**, 57002 (2019).
[25] K. Halterman, M. Alidoust, R. Smith, and S. Starr, Phys. Rev. B **105**, 104508 (2022).
[26] E. Strambini, M. Spies, N. Ligato, S. Ilic, M. Rouco, C. G. Orellana, M. Ilyn, C. Rogero, F. Bergeret, J. Moodera *et al.*, Nat. Commun. **13**, 2431 (2022).
[27] M. Silaev, A. Y. Aladyshkin, M. Silaeva, and A. Aladyshkina, J. Phys. Condens. Matter **26**, 095702 (2014).
[28] A. E. Schegolev, N. V. Klenov, I. I. Soloviev, A. L. Gudkov, and M. V. Tereshonok, Nanobiotechnol. Rep. **16**, 811 (2021).
[29] L. Fu, J. Club Condens. Matter Phys. (2021).
[30] T. W. Larsen, M. E. Gershenson, L. Casparis, A. Kringhøj, N. J. Pearson, R. P. G. McNeil, F. Kuemmeth, P. Krogstrup, K. D. Petersson, and C. M. Marcus, Phys. Rev. Lett. **125**, 056801 (2020).
[31] A. Gyenis, A. Di Paolo, J. Koch, A. Blais, A. A. Houck, and D. I. Schuster, PRX Quantum **2**, 030101 (2021).
[32] C. Schrade, C. M. Marcus, and A. Gyenis, PRX Quantum **3**, 030303 (2022).
[33] A. Maiani, M. Kjaergaard, and C. Schrade, PRX Quantum **3**, 030329 (2022).
[34] T. Fulton, L. Dunkleberger, and R. Dynes, Phys. Rev. B **6**, 855 (1972).
[35] E. M. Spanton, M. Deng, S. Vaitiekėnas, P. Krogstrup, J. Nygård, C. M. Marcus, and K. A. Moler, Nat. Phys. **13**, 1177 (2017).
[36] F. Nichele, E. Portolés, A. Fornieri, A. M. Whiticar, A. C. C. Drachmann, S. Gronin, T. Wang, G. C. Gardner, C. Thomas, A. T. Hatke, M. J. Manfra, and C. M. Marcus, Phys. Rev. Lett. **124**, 226801 (2020).
[37] I. Sochnikov, L. Maier, C. A. Watson, J. R. Kirtley, C. Gould, G. Tkachov, E. M. Hankiewicz, C. Brüne, H. Buhmann, L. W. Molenkamp, and K. A. Moler, Phys. Rev. Lett. **114**, 066801 (2015).

[38] M. Kayyalha, A. Kazakov, I. Miotkowski, S. Khlebnikov, L. P. Rokhinson, and Y. P. Chen, npj Quantum Mater. **5**, 7 (2020).
[39] F. Schindler, Z. Wang, M. G. Vergniory, A. M. Cook, A. Murani, S. Sengupta, A. Y. Kasumov, R. Deblock, S. Jeon, I. Drozdov *et al.*, Nat. Phys. **14**, 918 (2018).
[40] C. D. English, D. R. Hamilton, C. Chialvo, I. C. Moraru, N. Mason, and D. J. Van Harlingen, Phys. Rev. B **94**, 115435 (2016).
[41] G. Nanda, J. L. Aguilera-Servin, P. Rakyta, A. Kormányos, R. Kleiner, D. Koelle, K. Watanabe, T. Taniguchi, L. M. Vandersypen, and S. Goswami, Nano Lett. **17**, 3396 (2017).
[42] C. W. J. Beenakker, Phys. Rev. Lett. **67**, 3836 (1991).
[43] J. M. Martinis and K. Osborne, arXiv:cond-mat/0402415.
[44] B. I. Spivak and S. A. Kivelson, Phys. Rev. B **43**, 3740 (1991).
[45] J. A. Van Dam, Y. V. Nazarov, E. P. Bakkers, S. De Franceschi, and L. P. Kouwenhoven, Nature (London) **442**, 667 (2006).
[46] R. Delagrange, R. Weil, A. Kasumov, M. Ferrier, H. Bouchiat, and R. Deblock, Phys. Rev. B **93**, 195437 (2016).
[47] S. Hart, Z. Cui, G. Ménard, M. Deng, A. E. Antipov, R. M. Lutchyn, P. Krogstrup, C. M. Marcus, and K. A. Moler, Phys. Rev. B **100**, 064523 (2019).
[48] R. Allub, C. Wiecko, and B. Alascio, Phys. Rev. B **23**, 1122 (1981).
[49] J. C. Estrada Saldaña, A. Vekris, G. Steffensen, R. Žitko, P. Krogstrup, J. Paaske, K. Grove-Rasmussen, and J. Nygård, Phys. Rev. Lett. **121**, 257701 (2018).
[50] See Supplemental Material at http://link.aps.org/supplemental/10.1103/PhysRevLett.129.267702, which includes Refs. [44,48,49,51–55], for details on the model for the quantum dot interferometer, the diode efficiency optimization, the fractional Shapiro steps, and the temperature dependence of the Josephson diode effect.
[51] C. Schrade, S. Hoffman, and D. Loss, Phys. Rev. B **95**, 195421 (2017).
[52] M. J. Rančić, S. Hoffman, C. Schrade, J. Klinovaja, and D. Loss, Phys. Rev. B **99**, 165306 (2019).
[53] M.-S. Choi, M. Lee, K. Kang, and W. Belzig, Phys. Rev. B **70**, 020502(R).
[54] C. Karrasch, A. Oguri, and V. Meden, Phys. Rev. B **77**, 024517 (2008).
[55] M. Tachiki, T. Koyama, and S. Takahashi, Prog. Theor. Phys. Suppl. **108**, 297 (1992).
[56] W. Stewart, Appl. Phys. Lett. **12**, 277 (1968).
[57] D. McCumber, J. Appl. Phys. **39**, 3113 (1968).
[58] J. Park, Y.-B. Choi, G.-H. Lee, and H.-J. Lee, Phys. Rev. B **103**, 235428 (2021).
[59] J. C. Cuevas, J. Heurich, A. Martín-Rodero, A. Levy Yeyati, and G. Schön, Phys. Rev. Lett. **88**, 157001 (2002).
[60] R. Duprat and A. Levy Yeyati, Phys. Rev. B **71**, 054510 (2005).
[61] M. Chauvin, P. Vom Stein, H. Pothier, P. Joyez, M. E. Huber, D. Esteve, and C. Urbina, Phys. Rev. Lett. **97**, 067006 (2006).
[62] X. Gu, A. F. Kockum, A. Miranowicz, Y. Liu, and F. Nori, Phys. Rep. **718**, 1 (2017).
[63] Y. V. Fominov and D. S. Mikhailov, Phys. Rev. B **106**, 134514 (2022).